Acid Stimulation in Single Carbonate Fractures with Heterogeneous Apertures

Haoran Xu[1], Jingru Cheng[1], Zhihong Zhao[1(✉)], Tianyi Lin[2], and Sicong Chen[1]

[1] Department of Civil Engineering, Tsinghua University, Beijing 100084, China
zhzhao@tsinghua.edu.cn
[2] Beijing Institute of Geothermal Research, Beijing 100012, China

Abstract. The service life of geothermal wells is affected by the reservoir permeability. Acid fracturing has been utilized to improve productivity in fractured carbonate geothermal reservoirs recently. A modeling method for the coupled thermal-hydro-mechanical-chemical (THMC) process during acid fracturing is developed. In a benchmark test, the effect of aperture heterogeneity on the efficiency of acid fracturing in geothermal reservoirs is examined. The results show that the acid flow and aperture increase exhibit significant anisotropy in the heterogeneous characteristics. Based on a field test of acid fracturing in a geothermal well, Tongzhou, Beijing, we use the built three-dimensional fractured porous reservoir model to simulate the process of acid fracturing. The agreement between the simulation and the field test data demonstrate that the proposed modeling method is capable of simulating acid fracturing in fractured carbonate geothermal reservoirs.

Keywords: Fractured carbonatite reservoir · Heterogeneity · Acid fracturing · Coupled THMC process · Finite element method

1 Introduction

Geothermal wells may suffer from disappointing injectivity and productivity with time or right from the start, and hydraulic or acid fracturing treatment to improve the wells' performance have been developed based on the experiences in the oil and gas industry. The application of the correct well stimulation technique in an optimum manner is helpful to establish and maintain the maximum energy capacity of geothermal wells. It is known that acid fracturing is an effective method for the stimulation of carbonate geothermal reservoirs. Selecting the optimal flow rate is an important task in reservoir stimulation, in order to achieve the maximum increase in permeability for a given amount of reactant. If the acid is injected too slowly, significant dissolution occurs only at the inlet, and the permeability of the system remains almost unchanged. At the other extreme of high injection velocities dissolution tends to be uniform throughout the whole fracture. Note that the optimized injection rate is affected by many factors including rock physical properties, acidizing conditions, as well as in-situ stress and temperature conditions. Numerous numerical models have been developed to simulate the reactive flow in fractured rocks, and they can consider the coupled processes of

M. Barla et al. (Eds.): IACMAG 2021, LNCE 126, pp. 1041–1049, 2021.
https://doi.org/10.1007/978-3-030-64518-2_124

fluid flow, heat transfer, and reactive transport, as well as the heterogeneity in fracture geometrical and mineral properties (Yuan et al. 2016; Liu et al. 2017; Ma et al. 2018; Jones and Detwiler 2019). However, there are few modeling methods which can simulate the acid fracturing in fractured carbonate geothermal reservoirs considering the fully coupled thermal-mechanical-hydrological-chemical processes.

The main aim of this study is to develop a fully coupled thermo-hydro-mechanical-chemical (THMC) model for acid fracturing treatment in carbonate geothermal reservoirs containing a single fracture. The fracture is surrounded by three-dimensional low permeable rock matrix. Both a benchmark example and a field test are presented.

2 Numerical Method

Governing equations for fluid flow, reactive transport, heat transfer and solid mechanics in fracture and matrix are presented below. The fracture can be conceptualized as a set of parallel plates by assuming that the fracture midsurface is planar and that the variation in aperture is small relative to its mean value. The acid flow in rock fractures can be described as,

$$b\rho S_f \frac{\partial p_f}{\partial t} + \nabla \cdot \left(b\rho \mathbf{u}_f\right) = bq_m \tag{1a}$$

$$\mathbf{u}_f = -\frac{b^2}{12\mu F_T}\left(\nabla p_f + \rho \mathbf{g}\right) \tag{1b}$$

where b is the real-time aperture altered by mechanical and chemical processes, ρ is the fluid density, p_f is the aperture-averaged fluid pressure, S_f is the storage coefficient of fracture, $\mathbf{u}_f$ is the flow velocity vector, q_m is the lateral exchange of fluid between the fracture and the matrix, t is time, μ is the dynamic viscosity, F_T is an empirical parameter, $\mathbf{g}$ is the gravitational acceleration, F_T is an empirical parameter that accounts the non-laminar flow.

The fluid flow in porous rock matrix are normally regarded as laminar flow, which is described by the continuity equation and Darcy's Law.

$$\rho S_r \frac{\partial p_r}{\partial t} + \nabla \cdot (\rho \mathbf{u}_r) = q_m \tag{2a}$$

$$\mathbf{u}_r = -\frac{k}{\mu}(\nabla p_r + \rho \mathbf{g}) \tag{2b}$$

where $\mathbf{u}_r$ is the Darcy velocity in the rock matrix, k is the permeability of the rock matrix, p_r is the fluid pressure in the rock matrix, S_r is the storage coefficient, which is a function of porosity (ϕ), Biot-Willis coefficient (α_B), fluid bulk modulus (K_f), and drained bulk modulus (K_d).

$$S_r = \frac{\phi}{K_f} + (\alpha_B - \phi)\frac{1-\alpha_B}{K_d} \tag{3}$$

The coupling between the fluid flow and mechanical displacement is considered as,

$$\rho S_r \frac{\partial p_r}{\partial t} + \nabla(\rho \mathbf{u}_r) = -\rho \alpha_B \frac{\partial \varepsilon_{vol}}{\partial t} + q_m \tag{4}$$

where ε_{vol} is the average volumetric strain of the rock matrix. The coupling between flow through fracture and rock matrix is incorporated by,

$$bq_m = \rho\left(u_{rz}|_{z=-b/2} - u_{rz}|_{z=b/2}\right) \tag{5}$$

where z = $\pm b/2$ represent the interfaces between the fracture and the rock matrix.

The rate (R^i_r) of the chemical reaction between carbonate rocks and the acid is a function of acid concentration and ambient temperature,

$$R^i_r = k_f C_i^{n_a} \tag{6a}$$

$$k_f = A_f e^{-\frac{E_a}{RT}} \tag{6b}$$

where k_f is the reaction rate coefficient that is described by the Arrhenius law (Eq. 7), C_i is the acid concentration, n_a is the order of reaction, A_f is the preexponential factor, E_a is the activation energy, R is the molar gas constant, T is temperature.

The reactive transport equation in fracture is,

$$b \cdot [\frac{\partial\left(C^f_i\right)}{\partial t} + \mathbf{u}_f \cdot \nabla C^f_i] - \nabla \cdot \left(bD^i_{ef} \nabla C^f_i\right) = b \cdot [R^i_f + S_i] \tag{7}$$

where $C^f{}_i$ is the solute concentration in the fracture (i = HCl or $CaCl_2$), $D^i{}_{ef}$ is the solute diffusion coefficient in the fracture, S_i is the solute flux from the fracture to the rock matrix, R^i_f is the reaction rate in the fracture.

The reactive transport equation in porous rock matrix is,

$$C^r_i S_r \frac{\partial p_r}{\partial t} + \mathbf{u}_r \cdot \nabla C^r_i - \nabla \cdot \left(D^i_{er} \nabla C^r_i\right) = R^i_r \phi \tag{8}$$

where $C^r{}_i$ is the solute concentration in the rock matrix (i = HCl or $CaCl_2$), $D^i{}_{er}$ is the solute diffusion coefficient in the matrix, R^i_r is the reaction rate in the rock matrix.

Dong et al. (2002) showed that almost all leakoff acid flows out of the fracture without reacting with the fracture walls, and that all acid transported by diffusion reacts with the formation at the fracture walls. With these assumptions, the change of the fracture width is represented by,

$$\frac{\partial b_c}{\partial t} = 2k_g \overline{C}^f_{HCL} \frac{\beta}{\rho_r(1-\phi)} \tag{9}$$

where ρ_r is the density of rock matrix, C^f_{HCL} is the aperture-averaged acid concentration, k_g is the apparent mass-transfer coefficient, β is acid dissolving power.

Considering fluid flow and chemical reactions, heat transport in the fracture can be described as,

$$b[\rho C \frac{\partial T}{\partial t} + \mathbf{u}_f \rho C \cdot \nabla T] - \nabla \cdot (b\lambda \nabla T) = bQ^f_{chem} + \mathbf{n} \cdot \mathbf{q} \tag{10}$$

where C is the specific heat capacity of the fluid, λ is the thermal conductivity of the fluid, $\mathbf{n}\cdot\mathbf{q}$ is the heat from the matrix into the fracture, Q^f_{chem} is the heat source induced by chemical reactions.

Heat transport in the rock matrix can be described as,

$$(\rho_i C_i)_{eff} \frac{\partial T}{\partial t} + \mathbf{u}_r \rho C \cdot \nabla T - \nabla \cdot \left(\lambda_{eff} \nabla T\right) = Q^r_{chem} \tag{11}$$

where $(\rho_i C_i)_{eff}$ is the volumetric mean of the heat capacity, λ_{eff} is the volumetric mean of the heat conductivities of the rock and the acid, Q^r_{chem} is the heat source derived from chemical reaction.

Shear dilation and elastic displacement are considered to affect the fracture aperture. Elastic layer is complemented to simulate the fracture displacement, given as,

$$\sigma'_n = \sigma_n - p_f = k_n u_n \tag{12a}$$

$$\sigma_s = k_s u_s \tag{13b}$$

where σ_n and σ_s are the normal and shear stresses, σ'_n is the effective normal stresses, k_n and u_n are the normal stiffness and normal displacement, k_s and u_s are the shear stiffness and shear displacement.

The shear-induced dilation can be described as,

$$u_d = \begin{cases} 0 & u_s \le u_p \\ u_s \tan \varphi_d & u_p \le u_s \le u_{cs} \\ u_{cs} \tan \varphi_d & u_s \ge u_{cs} \end{cases} \tag{13}$$

where u_p is the shear displacement at the peak shear stress, u_{cs} is the shear strain at the critical stress, φ_d is the dilation angle.

Therefore, the fracture aperture mediated by the mechanical and chemical processes becomes,

$$b = b_0 + b_c + u_n + u_d \tag{14}$$

Thermo-poro-elasticity typically describe the linked interactions among fluid, temperature and deformation in porous rock matrix. The relationship between stress tensor ($\boldsymbol{\sigma}$), strain tensor ($\boldsymbol{\varepsilon}$), and pore fluid pressure (p_f) is,

$$\boldsymbol{\sigma} = \mathbf{C}_{kr}(\boldsymbol{\varepsilon} - \varepsilon_T) - \alpha_B p\mathbf{I} \tag{15a}$$

$$\varepsilon_T = \alpha_T\left(T - T_{ref}\right) \tag{15b}$$

$$p = M(\zeta - \alpha_B\phi) \tag{15c}$$

where $\mathbf{C}_{kr}$ is the elasticity matrix measured under drained condition. Thermal strain (ε_T) is expressed in terms of the coefficient of thermal expansion (α_T) and the change from an initial temperature (T_{ref}), M is the Biot modulus, which is the inverse of the storage coefficient, ζ is the variation of fluid content.

Navier's equations for a solid in equilibrium under purely gravitational load is,

$$-\nabla\sigma = \rho_{av}\mathbf{g} = [\rho_f\phi + \rho_r(1-\phi)]\mathbf{g} \tag{16}$$

where ρ_{av} represents the average density.

The reservoir is simulated as a three-dimensional (3D) domain including one single fracture, and the 3D domains are discretized into finite tetrahedron elements. When the domain discretization using tetrahedron elements and the time discretization using backward Euler time integration scheme are completed, the linear system is solved using parallel direct sparse solver interface in COMSOL.

3 Case Studies

3.1 Benchmark Example

A benchmark reservoir model containing a vertical stimulation well and a single horizontal fracture with was built (Fig. 1), and the effect of aperture heterogeneity on acidizing efficiency was examined. The numerical reservoir model was 300 m long, 300 m wide, and 50 m high, which was used to represent the carbonate geothermal reservoir at a depth of about 3 km. To study the acidizing process in heterogeneous fractured geothermal reservoir, the fracture was divided into 900 domains. We built two models with different initial fracture apertures: 1) heterogeneous model: the initial fracture apertures followed the log-normal distribution with the mean fracture aperture of 1 mm, the standard deviation of 0.25 mm, and the spatial correlation length of 15 m; 2) uniform model: the uniform initial aperture was 1mm. A tetrahedron mesh is used in this study, which has a characteristic element length of about 0.1 to 20 m, resulting in about 165,000 elements and 30,000 nodes. The initial and boundary conditions pertain to the general condition of the carbonatite reservoir at the depth of 3 km. In-situ stresses σ_v = 90 MPa, σ_H = 50 MPa, and σ_h = 40 MPa were applied on the model boundaries. The initial temperature of the reservoir was 80 °C, and the temperature of the injected acid was 20 °C. Acidizing was performed by injecting 28% acid solution (acid concentration of 8075 mol/m^3) through the stimulation well in the fractured

reservoir. Under the pressure difference between the stimulation well and the reservoir, the reactive acid flowed through the fracture and induces aperture alteration. The period for acidizing was 120 min and was divided into three stages, each of which lasted for 40 min. The pumping rates of the three stages were 2.0, 3.0 and 4.0 m^3/min. Respectively. The model parameters are listed in Table 1.

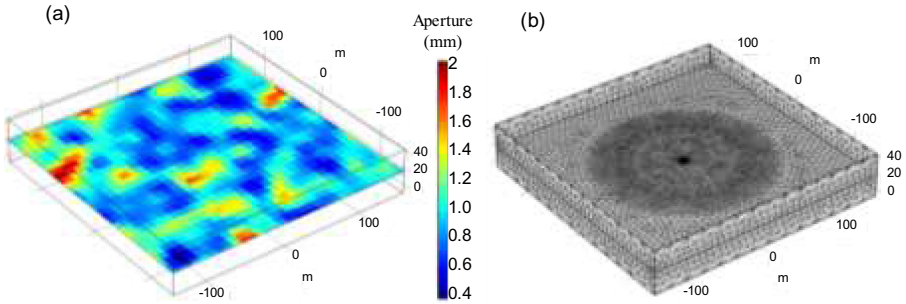

Fig. 1. The numerical model (a) and the mesh (b) of the benchmark example.

Table 1. Model parameters

Category	Parameters (unit)	Values
Geometry	Wellbore radius (m)	0.02
Rock matrix	Density ρ_r (kg/m^3)	2600
	Young's modulus (GPa)	50
	Poisson's ratio	0.25
	Initial porosity ϕ	0.05
	Biot coefficient α_B	0.1
	Permeability k (m^2)	2.96e-14
	Thermal expansion coefficient α_T (1/K)	2e-6
	Specific heat capacity C_r (J/(kg·K))	880
	Thermal conductivity λ_r (W/(m·K))	1.57
Fractures	Normal stiffness k_n (GPa/m)	17
	Shear stiffness k_s (GPa/m)	9
	Acid dissolving power β	1.3699
	Angle of dilation φ_d (°)	12.2
	Tangential displacement for u_p (mm)	0.54
	Critical value of shear displacement u_{cs} (mm)	2
	Storage coefficient of fracture S_f (Pa^{-1})	1.0e-8
Acid solution	Pump rate (m^3/min)	2.0/3.0/4.0
	Initial temperature (K)	293.15
	Density ρ (kg/m^3)	1192
	Specific heat capacity C (J/kg)	4182

(*continued*)

Table 1. (*continued*)

Category	Parameters (unit)	Values
	Compressibility $1/K_f$ (1/Pa)	3.0303e-10
	Diffusion coefficient D^H_{ef} (m^2/s)	1.15e-10
	Initial concentration C_{HCL} (mol/m^3)	8750
	Empirical parameter F_T	1.8
Chemical reaction	Reaction order n_a	0.6
	Forward activation energy E_a (J/mol)	53208.77
	Preexponential factor A_f (mol/L)$^{-na}$·mol/(s·m^3)	27529.13

With the injection, the aperture altered by chemical reaction increased gradually in both heterogeneous model (Fig. 2 a, b, c) and uniform model (Fig. 2 d, e, f). The heterogeneous model and the uniform model had significantly different aperture enhancement patterns, i.e., the acid flow and aperture increasement exhibit significant anisotropy in the heterogeneous fractures (heterogeneous model). The distribution of H^+ concentration in the fractures of heterogeneous model and uniform model also showed different patterns (Fig. 3b, e). Neither the fluid viscosity (Fig. 3a and d) nor the temperature (Fig. 3c and f) was significantly affected by the heterogeneous apertures.

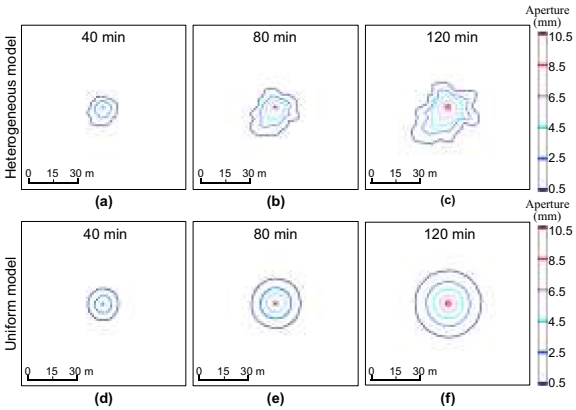

Fig. 2. Comparison of the aperture enhancement patterns between models with the heterogeneous apertures (upper row) and a uniform initial aperture (low row) at different stages. Note that the central area of 100 × 100 m^2 is plotted.

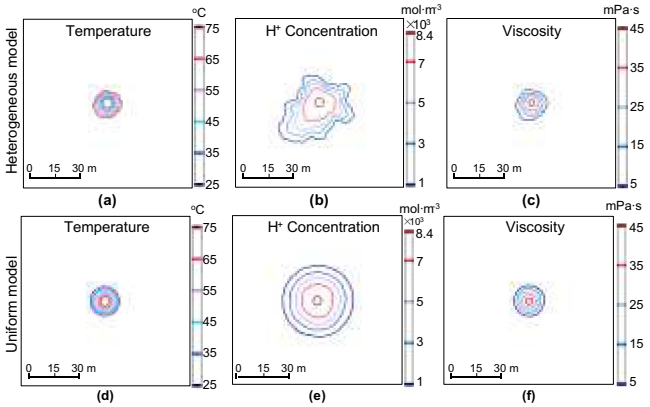

Fig. 3. Comparison of the acid temperature (a and d), H+ concentration (b and e) and viscosity (c and f) between models with the heterogeneous apertures (upper row) and a uniform initial aperture (low row) at 120 min. Note that the central area of 100 × 100 m^2 is plotted.

3.2 Case Study

A geothermal well was drilled in Tongzhou, Beijing from March to December 2018 at a depth of 3000 m. From the field test data, the injection pressure of the acid was 5–6 MPa, and was lowered to 1 MPa before injecting the after-pad fluid. The fluid utilized in acid fracturing is 20% hydrochloride acid. As the diameter of the downhole tube is 73 mm, wellbore diameter is simplified as 100 mm in the simulation. The reservoir is mainly composed of dolomite, and the acid concentration at the surface of the rock was calculated using the following surface concentration model (Li et al. 1993),

$$\frac{\partial C_{HCL}^{wall}}{\partial t} = k_g(\overline{C}_{HCL}^{f} - C_{HCL}^{wall}) - k_f(C_{HCL}^{wall})^{n_a} \tag{17}$$

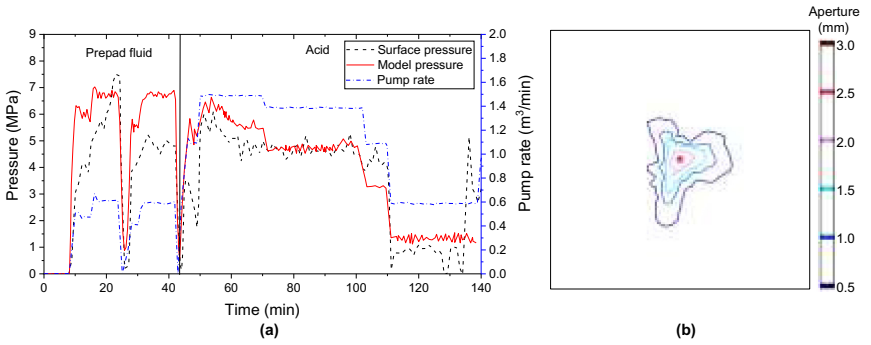

Fig. 4. The modeled pressure (a) and apertures (b) for the case study of acid fracturing in Tongzhou, Beijing.

Under the same pump rate as the field test, the simulation gave the similar surface pressure as the field test (Fig. 4). After 139 min of fracturing construction the maximum fracture half-length is about 65 m (Fig. 4).

4 Conclusion

A modeling method for the coupled thermal-hydro-mechanical-chemical (THMC) process during acid fracturing is developed, and a benchmark example and a field test are presented, which demonstrate that the proposed modeling method is capable of simulating acid fracturing in fractured carbonate geothermal reservoirs.

Acknowledgements. The activity presented in the paper is part of the National Key R&D Program of China (No. 2019YFB1504103) and the National Natural Science Foundation of China (No. 51779123, 51739006).

References

Dong, C., Zhu, D., Hill, A.: Modeling of the acidizing process in naturally fractured carbonates. SPE J. **7**, 400–408 (2002)

Jones, T.A., Detwiler, R.L.: Mineral precipitation in fractures: using the level-set method to quantify the role of mineral heterogeneity on transport properties. Water Resour. Res. **55**, 4186–4206 (2019)

Li, Y., Sullivan, R.B., de Rozieres, J., Gaz, G.L., Hinkel, J.J.: An overview of current acid fracturing technology with recent implications for emulsified acids. In: SPE Annual Technical Conference and Exhibition. Society of Petroleum Engineers (1993)

Liu, P., Yao, J., Couples, G.D., Ma, J., Huang, Z., Sun, H.: Modelling and simulation of wormhole formation during acidization of fractured carbonate rocks. J. Petrol. Sci. Eng. **154**, 284–301 (2017)

Ma, G., Chen, Y., Jin, Y., Wang, H.: Modelling temperature-influenced acidizing processes in fractured carbonate rocks. Int. J. Rock Mech. Min. Sci. **105**, 73–84 (2018)

Yuan, T., Ning, Y., Qin, G.: Numerical modeling and simulation of coupled processes of mineral dissolution and fluid flow in fractured carbonate formations. Transp. Porous Media **114**, 747–775 (2016)